Journal of Magnetism and Magnetic Materials 570 (2023) 170441

Contents lists available at ScienceDirect

Journal of Magnetism and Magnetic Materials

journal homepage: www.elsevier.com/locate/jmmm

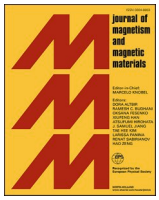

Magneto-mechanical properties of anisotropic magnetorheological elastomers with tilt angle of magnetic chain under compression mode

Leizhi Wang [a,b], Zhaobo Chen [a,*], Like Jiang [b], Li Cheng [b]

[a] School of Mechatronics Engineering, Harbin Institute of Technology, Harbin 150001, PR China
[b] Department of Mechanical Engineering, The Hong Kong Polytechnic University, Hong Kong Special Administrative Region

ARTICLE INFO

Keywords:
Anisotropic MREs
Compression mode
Tilt angle
Magneto-mechanical properties

ABSTRACT

Characterization of mechanical properties of magnetorheological elastomers (MREs) is essential for the design of smart materials and devices with customized features and functionalities. While the properties of MREs under shear mode have been extensively researched, MREs with tilt angle under compression mode have been less exploited. In this study, a magneto-mechanical model of anisotropic MREs is established based on magnetic dipole theory and energy method considering the reconfiguration effect of compressive strain on the microstructure of the magnetic chain. This leads to the provision of a dynamic magneto-mechanical model of the anisotropic MREs, incorporating the magneto-induced mechanical model, by using the robust fitting method. Experiments were conducted to assess the force–deflection (stress–strain) characteristics of MREs with tilt angle under compression mode, subject to the regulation of the tilt angle of magnetic chain, magnetic flux density, and mass fraction of magnetic particles. The magnetic-induced modulus, obtained from the theoretical model, is experimentally verified through magneto-mechanical testing, alongside an analysis on the dynamic mechanical properties under different dynamic strain amplitudes and frequencies. The mean square error (MSE) in terms of magneto-mechanical storage modulus in the robust fitting ranges from 2.73% to 10.86%. Experimental results also show that the range of magneto-induced stress (typically from 178 KPa to 74.6 KPa) decrease when the tilt angle of the magnetic chain increases (from 15° to 25°) corresponding to 60% mass fraction. The compression strain of the anisotropic MREs, affecting both the spacing of adjacent magnetic particles and the tilt angle of magnetic chain, causes significant changes in the magnetic-induced modulus. In addition, the hysteresis loops under different deformation (Mullins effect) show an increasing energy dissipation with decreasing tilt angle.

1. Introduction

Magnetorheological elastomers (MREs) are widely used as "smart" materials in dynamic vibration absorbers [1–4], sensors [5–7], grippers for intelligent robots [8,9], magnetically driven soft robots [10], and wearable electronic devices [11,12] etc. MREs originate from the family of magnetorheological materials. This MREs material exhibits controllable mechanical properties responding to an external magnetic field. In addition, the electrical conductivity of different MREs is subjected to mechanical strain and magnetic flux to achieve signal receive and control of intelligent device [13]. The magneto-mechanical property of MREs is fundamental for the functional and structural design of smart devices. The research on magneto-mechanical properties of MREs is mainly from two aspects: theoretical model and material design. The reviews [14,15] of syntheses and magneto-mechanical characterization of MREs summarized different testing methods (dynamic or quasi-static) and fabrication technical, which present field-controllable properties of MREs.

Various models were proposed to characterize magneto-mechanical properties of anisotropic and isotropic MREs. The basis of the theoretical model adopts the magnetic dipole model [16,17] for analyzing the magneto-induced modulus. The expressions of the magnetic induction energy and elastic strain energy in the energy method is parsed to get the constitutive relation [18,19]. A great deal of research has been done on the theoretical model of the magneto-mechanical shear behavior, and a brief overview is given below. A two-parameter dipole moment semi-empirical model [16] was established through experimental tests. The theoretical stress–strain relationship was derived to describe shear modulus relation with dipoles distance and particle diameter [17]. Meanwhile, a stress–strain relationship model of quasi-static MRE shear

* Corresponding author.
E-mail address: chenzb@hit.edu.cn (Z. Chen).

https://doi.org/10.1016/j.jmmm.2023.170441
Received 5 October 2022; Received in revised form 10 January 2023; Accepted 20 January 2023
Available online 6 February 2023

[18] was developed to analyze the two stress sources, which contain the interaction of magnetic particles and rubber matrix and magnetic dipole moment. In addition, the MREs nonlinear response of 2D pure shear and 3D axisymmetric shear under magnetic field was also studied to validate the proposed general criterion [20] based on the general criterion of bifurcation and stability theory. The model describing MREs with wrapped nanoparticles of soft shell was proposed to predict the relationship of magnetic parameters and shear modulus [21]. The general dipole model could not accurately predict the shear modulus of the complex microstructure. In order to the analysis of the magneto-induced model more accurate and reliable, a variety of microstructure morphologies are considered as following literatures. The mechanical model of anisotropic MREs with straight and waveform magnetic chain [19] was proposed. The shear stiffness formula was derived from the static magnetic energy and shear strain energy when the material was subjected to shear deformation. The magnetic-mechanical coupling model of MRE materials under large pre-stress conditions is proposed [22], which analyzed the effect of pre-stress on magnetic-induced shear storage modulus. The magnetic-induced mechanical model for estimating shear modulus based on magneto-static deformation was proposed [23] by considering three different forms of spatial distribution including chain, plane and isotropic. A magneto-elastic energy storage model [24] was proposed depending on the microstructure in terms of the mean deformation gradient and magnetic field, which considers magnetic dipole interaction and finite strain effect in a homogenized framework. The mechanical model of finite column [25] was proposed based on viscoelasticity to predict the performance of MREs under shear behavior.

In addition, there are studies based on the magneto-mechanical properties under compression [26–29] or tensile [30,31] behavior, which proposed some magneto-mechanical model. The static compressive magneto-mechanical properties of MREs [26] under magnetic field (parallel and perpendicular to the chain direction) was studied for the performance of magneto-static modulus. The large-strain behavior [32] of isotropic and anisotropic MREs was characterized experimentally under uniaxial compression. The linear viscoelastic region [33] in compression mode was studied in high frequencies (200 Hz). Furthermore, the MR properties of isotropic and anisotropic MREs experimentally under dynamic compression was analyzed, considering magnetic particle fraction, excitation frequency, and strain amplitude in six parameters empirical models [28]. The magneto-induced mechanical properties of MREs in dynamic compression mode was further developed considering large pre-strain [29]. The experimental results show that the storage modulus of relative MR calibration at 20% large strain increased by 188.32% for isotropic MRE and the anisotropic MRE increased by 216.24%. The proposed MREs with flax fibers [31] have superior mechanical and conductivity properties. The magnetic-induced mechanical properties in compression behavior was investigated revealing a smaller plastic deformation and energy absorption efficiency. Mechanical characterization of the above magnetorheological elastomers based on the injection molding manufacturing process. In recent research progress, 3D printing technology was used for developing special topology structures and hybrid MREs [34,35]. The various dot patterns MREs [36] consisting of isotropic, anisotropic and configurations inspired from basic lattice structure such as BCC and FCC. By rational design of the microarchitectures of porous structures and precise deposition of the multiple material phases in the space, many researches proposed architected materials with tailor-made mechanical properties under compression [37]. The research presents the effect of shape factor on compression mode dynamic properties of MRE by considering strain-rate and amplitude [38]. Moreover, a methodology was proposed for compensating for the magnetic force generated by electromagnets for accurate characterizations of MREs compression mode [39]. These proposed models describe magneto-mechanical properties of anisotropic MREs under compression mode, however, the magneto-mechanical model of the anisotropic MREs, presented for tilt angle of magnetic chain influenced by compressive deformation, haven't been suitable performed.

With the goal of enhancing magnetorheological properties, the magnetic chain angle in microstructure was concerned on the researches of magneto-mechanical properties of anisotropic MREs. The magneto-mechanical properties of anisotropic MREs are highly dependent on the internal microstructure of magnetic chains, which mainly contains the lattice of magnetic particles and the magnetic chain arrangement. The mechanism of microstructure design (tilt angle of magnetic chain) is used as the modulation of magnetorheological effect. The magnetic moments ratio is regarded as indirect parameter for anisotropic coefficient, which of horizontal and vertical directions for anisotropic MREs with different magnetic particle concentrations was characterized by using vibrating sample magnetometer (VSM) [40]. The microstructural effect of anisotropic MRE is influenced by the curing process of magnetic field and magnetic particle fraction of hybrid precursor. The results show that a critical concentration of magnetic particles makes the transformation of anisotropic magnetic chains to a more complex three-dimensional microstructure. Regardless of the mechanical behaviors, the microstructure of magnetic chains in anisotropic MRE is important for magneto-mechanical properties. The quasi-static and dynamic shear magnetic-induced properties of different magnetic chain angles [41]

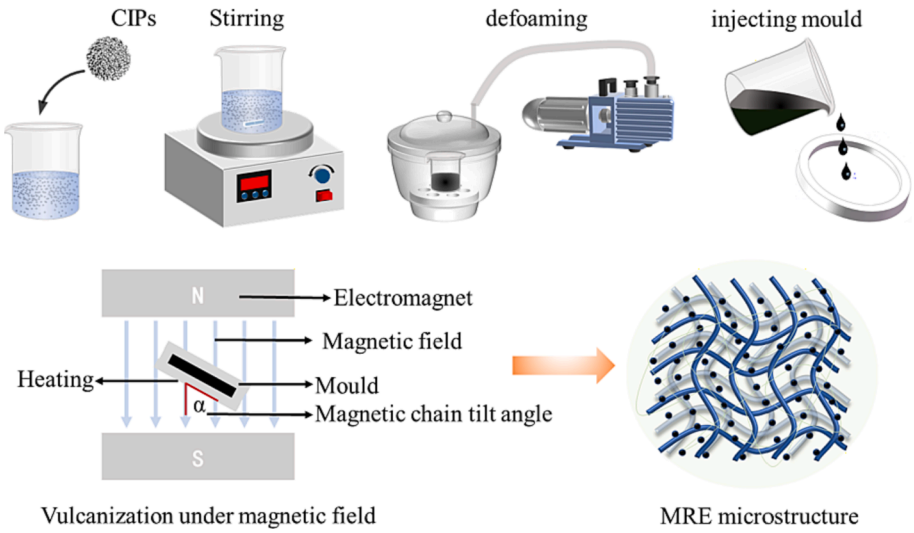

Fig. 1. Process flow chart of anisotropic MRE preparation.

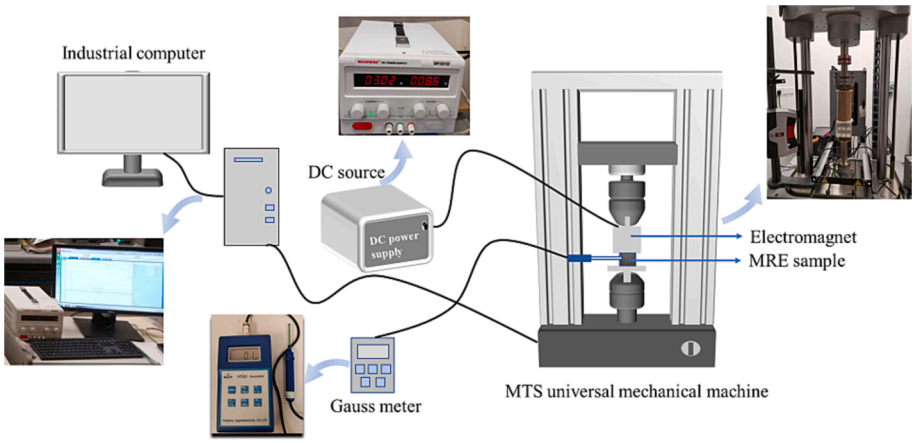

Fig. 2. The illustrations of magneto-mechanical test setup of anisotropic MREs under compression.

were investigated to propose the constitutive model describing shear magnetic-induced model. The anisotropic MREs with 45-degree magnetic chains synthesizing with different concentrations of silicone oil [42] were researched to discuss the dynamic shear viscoelastic magneto-mechanical properties. The iron micron-sized particles and magnetic chain angles of anisotropic MREs [43] were investigated for analyzing the shear dynamic mechanical properties of MREs, optimizing the particles size, shape and alignment. The above researches prove that the magneto-mechanical properties strongly depend on the microstructure, in particular on the particles used and their arrangement. While the magneto-mechanical properties of anisotropic MREs considering the effect of compressive deformation on the tilt angle of magnetic chains is less analyzed. Therefore, the magnetic-induced mechanical properties of anisotropic MREs with the tilt angle under quasi-static and dynamic compression is regarded as the key research object.

In this paper, the main content consists of three parts. Section 2 presents the customized electromagnetic coil with a compression head to experimentally characterize magnetic-induced mechanical properties of the anisotropic MREs. The special preparation procedure is that the precursor material was injected in an angular mold, placing on the center of the vertical magnetic field and heating the mold to accelerate vulcanization. Section 3 established theoretical magneto-mechanical model based magnetic dipole theory considering the compressive strain and tilt angle of magnetic chains. Section 4 discussed the theorical and experimental results of both static and dynamic mechanical property of anisotropic MREs with tilt angle. The coupling effect of the tilt angle and compressive strain on magnetic-induced modulus was revealed by using theorical and experimental methods. The Mullins effects present the variation of unloading path of hysteresis loop in anisotropic MREs with tilt angle. Owing to considerable strain amplitude and frequency, dynamic mechanical properties of the anisotropic MREs were evaluated for different tilt angles and CIPs mass fractions.

2. Material and experimental methods

2.1. MRE preparation

Magnetorheological elastomer samples with anisotropic thickness of 5 mm were prepared with 0, 15- and 25-degree magnetic chain tilt angle in spatial microstructure. The MRE samples with 40%, 60% and 80% mass fraction of magnetic particles in the corresponding tilt angles were prepared to study the magnetic-induced mechanical properties of anisotropic MREs under different magnetic flux density. The process flow of anisotropic MRE preparation is shown in Fig. 1. The magnetic particles were selected from carbonyl iron particles (CIPs, China Xindun alloy Corp.) with diameters ranging from 3 to 8 μm. The preparation of magnetorheological elastomers with tilt angles is divided into 4 steps. The first step was to prepare a well-mixed precursor by pouring the corresponding fraction of magnetic particles and the curing agent into a mixing cup with silicone rubber (Shin-Etsu Silicones, KE-2000ST) and placing it on a stirrer for constant speed mixing (60 rpm/min, 3 min). Secondly, the homogeneously mixed precursors were left in a negative pressure vacuum chamber (800 mmHg pressure) for 8 min. Then the defoamed precursors were slowly injected into the alloy mold with a circle groove (20 × 5 mm) by machine processing. Finally, the mold was sealed by the cover, which was heated by using thin plate heater of temperature at 80 ℃ in the gap of the magnetic field generator (China Dexing Electromagnetic DXSBV-100) that provide 1 T magnetic flux density for curing 20 min.

2.2. Experimental setup

The characterization of magneto-mechanical properties of MR elastomers in compression mode involves the application of an axial magnetic field and mechanical loading. Therefore, the cylindrical coils with a lamellar chuck at end of the coil core is designed to facilitate the clamping of the mechanical testing machine. A disc-shaped horizontal surface at the other end of customized coil has advantages on acting uniform and stable compressive loading and magnetic field on the anisotropic MREs. The coil was made of 1.6 mm diameter copper wire equipping a highly permeable pure iron core of cylindrical section of 20 mm diameter. A high strength coil skeleton was made of resin using 3D printing method. The customized electromagnetic coils are be clamped in the upper directions of the universal testing machine (UTM) to provide a flux density during the compression of MR elastomers as shown in Fig. 2. The electromagnetic coil is used for studying the effect of compression deformation on the magneto-mechanical properties revealing the nonlinear magneto-mechanical characteristics of anisotropic MREs. The Instron E10K testing instrument, for obtaining the stress/strain hysteresis loop, was used for calibrating the magnetic-induced modulus. The central control system of the UTM has been integrated in the industrial microcomputer. The load-acting beam is driven by an oil-free linear rotary motor, which has a linear load capacity of 10KN. The DC power supply (100 V, 20A) was used for providing the source of the clamped electromagnetic coils in Fig. 2. Magnetic flux density was measured by using a Gauss meter corresponding to controllable current. It is worth noting that the compression test under vertical magnetic field is different from the shear test. The magnetorheological elastomer is magnetized to produce magnetic force against the surface of the coil compression head, which displays negative value on the test software. Therefore, the load balance point needs to be recalibrated under a given magnetic field condition at different current. A uniform pre-strain value was selected as 0.1% after contacting the compression surface. The MRE samples were cut into a size of 8 mm

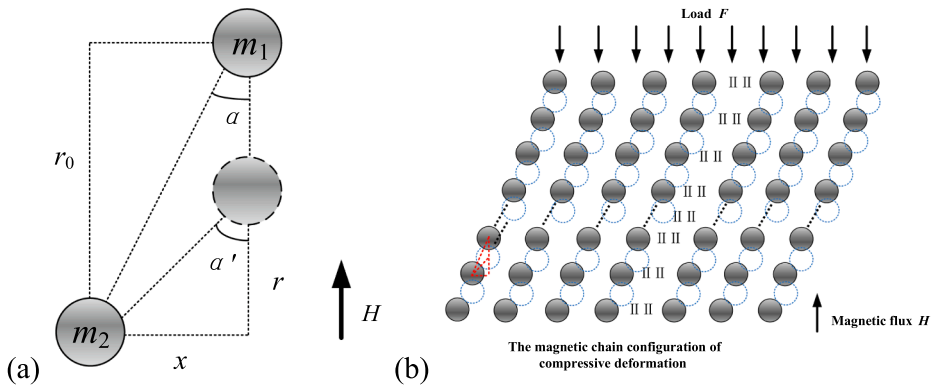

Fig. 3. (a) The subsystem of deformed dual magnetic dipoles; (b) The reconfiguration of magnetic chains under load and magnetic flux density.

× 8 mm × 5 mm to meet the ISO standard to meet the test requirements on MREs for magneto-mechanical coupling testing in compression.

3. Modelling and theory

The magnetic-induced mechanical model of anisotropic MREs with tilt angles of magnetic chain under compression was established by classical magnetic dipole theory and energy method. The improved quasi-static dipole model was proposed to analyze the regulation of magneto-induced compressive modulus considering both compressive strain and tilt angle of magnetic chain.

The most of MREs microscopic magnetic-induced model by using the magnetic energy model are derived from Rosensweig's theory. The improved double magnetic dipole model present that two adjacent particles (dipoles) in the same chain with tilt angle suffer the vertical magnetic field and compressive strain in Fig. 3. The interaction magnetic energy of the deformed double magnetic dipole m_1 and m_2 subsystem can also be expressed as:

$$E_{i,i+1} = \frac{1}{4\pi\mu_0\mu_l}\left[\frac{\vec{m}_i\cdot\vec{m}_{i+1}}{r^3} - \frac{3}{r^5}\left(\vec{m}_i\cdot\vec{r}\right)\left(\vec{m}_{i+1}\cdot\vec{r}\right)\right] \tag{1}$$

where r is spacing of adjacent magnetic dipoles of the same magnetic chain in the perpendicular magnetic field direction before deformation, μ_0 is the vacuum permeability, μ_l is the relative permeability of the matrix. i and $i+1$ represent the subscripts of the adjacent magnetic dipoles, and m_i is the magnetic dipole moment of the i th magnetic dipole of a certain magnetic chain under the external magnetic field. The magnetic field induced modulus of MRE under compression mode in [44] performs linear behavior with applied magnetic field. The linear magnetic field formulation used in both the model in the literature and the proposed model, as well as a sample prepared with similar mass fraction. Therefore, the magnetic dipole moment of single particle can be expressed as the Eqn. (2).

$$\vec{m}_i = \frac{4}{3}\pi a^3\mu_0\chi\overrightarrow{H_i} \tag{2}$$

$\overrightarrow{H_i}$ is a composite magnetic field (A/m); χ refers to the magnetic susceptibility of the particle and $\boldsymbol{a}$ its radius. The magnetic field of dipole i is influenced by both the applied magnetic field $\overrightarrow{H_0}$ and the magnetic field generated around the magnetic dipoles. Therefore, the Eqn. (3) of the magnetic field of magnetic dipole i after magnetization in MRE can be deduced as.

$$\overrightarrow{H_i} = \overrightarrow{H}_0 + 2\sum_{j=1}^{n}\frac{3\vec{r}\left(\vec{r}_j\cdot\vec{m}_j\right) - \vec{m}_j}{4\pi\mu_0 r_j^3} \tag{3}$$

Here we denote the magnetic dipoles around dipole i in the chain uniformly as the subscript variable parameter j; m_j is the magnetic dipole moment of magnetic particle j; r_j is the distance between magnetic particles i and j; $\vec{r}_j$ is the unit vector in its direction. When considering only the interaction between magnetic particles in the chain, assume that the distance between each particle is equal. r denotes the average distance between two particles, so there is $r_j = jr$. The magnetic dipole moment of the composite magnetic field can be expressed as Eqn. (4).

$$\vec{m}_i = \frac{4}{3}\pi a^3\mu_0\chi\left[\overrightarrow{H_0} + 2\sum_{j=1}^{n}\frac{3\vec{r}\left(\vec{r}_j\cdot\vec{m}_j\right) - \vec{m}_j}{4\pi\mu_0\mu_l(jr)^3}\right] \tag{4}$$

Assuming that each particle has the same magnetic dipole moment that we have $\boldsymbol{m_i} = \boldsymbol{m_j} = \boldsymbol{m}$.

$$\vec{m}_i = \frac{4}{3}\pi a^3\mu_0\chi\overrightarrow{H_0}\left[\frac{1}{1-(4/3)\chi\xi(a/r)^3}\right] \tag{5}$$

In the Eqn. (5), $\xi = \sum_{\infty}^{j=1}\frac{1}{j^3} \approx 1.202$. Consider the interaction energy between two magnetic dipoles in a magnetic chain system, Eqn. (6) represents the magnetic energy of the double dipoles subsystem.

$$E_i = \sum_{i\neq j}E_{ij} = 2\sum_{i=1}^{n}E_{ij} = 2\xi\frac{|m|^2}{4\pi\mu_0}\left[\frac{1-3\cos^2\alpha'}{r^3}\right] \tag{6}$$

In the Eqn. (6), α' present the angle of MRE microstructure magnetic chain after compression deformation; r_0 is the original spacing of adjacent magnetic dipoles in the same magnetic chain; r is the compressive deformed spacing of adjacent magnetic dipoles; and × is the spacing in horizontal direction of adjacent magnetic dipoles in the same magnetic chain. The microstructural parameters of the dual magnetic dipole subsystem are shown in Fig. 3(a) and the reconfiguration of magnetic chain under load and magnetic flux density is present in Fig. 3(b).

The microstructure of the dual magnetic dipole subsystem is analyzed due to the compression effect. The strain expression can be deduced from the correlation between strain and magnetic dipole spacing $r = r_0(1+\varepsilon)$. According the compression strain $\varepsilon = r/r_0 - 1$, the relationship of the subsystem parameters before and after deformation can be obtained as,

$$\cos^2\alpha' = \frac{r_0^2(1+\varepsilon)^2}{r_0^2(1+\varepsilon)^2 + x^2} \tag{7}$$

From the original microstructure Eqn. (8) of the dual magnetic dipole subsystem, we can conclude the total magnetic interaction energy of the subsystem in Eqn. (9).

$$\tan\alpha = \frac{x}{r_0} \tag{8}$$

$$E_i = 2\xi \frac{|m|^2\left[\tan^2\alpha - 2(1+\varepsilon)^2\right]}{4\pi\mu_0 r_0^3(1+\varepsilon)^3\left[(1+\varepsilon)^2+\tan^2\alpha\right]} \tag{9}$$

The following equation converting the mass fraction to the equivalent volume fraction is used in the calculation of the magneto-mechanical model.

$$\phi = \frac{V_p}{V_s+V_p} = \frac{\varphi\rho_s}{(1-\varphi)\rho_p+\varphi\rho_s} \tag{10}$$

where ϕ presents the volume fraction, and φ the mass fraction; ρ_s donates the density of silicone rubber ($\rho_s = 1.09$ g/cm^3) provided by the Shin-Etsu and ρ_p donates the density of carbonyl iron particles ($\rho_p = 4.5$ g/cm^3) provided by China Xindun Alloy Corp. The volume fractions corresponding to all prepared samples were listed to the parameter columns in Table 2.

Therefore, the macroscopic magnetic energy of the finite volume MRE can be expressed as Eqn. (11).

$$E_T = \frac{\phi V}{4/3\pi a^3 * 2} E_i \tag{11}$$

Then the magnetic energy density function is present as Eqn. (12)

$$W_m = \frac{E_T}{V} = \frac{3\phi}{8\pi a^3}E_i = \frac{3\xi\phi|m|^2}{16\pi^2 a^3\mu_0 r_0^3}\cdot\frac{\tan^2\alpha - 2(1+\varepsilon)^2}{(1+\varepsilon)^3\left[(1+\varepsilon)^2+\tan^2\alpha\right]} \tag{12}$$

The magneto-induced stress under compression in Eqn. (13) is deduced by the partial derivative of magnetic energy density function to compressive strain.

$$\sigma_m = \frac{\partial W_m}{\partial\varepsilon} = \frac{-0.304P(A+B\varepsilon+C\varepsilon^2+D\varepsilon^3+(8\xi\chi a-90r_0)\cdot\varepsilon^4-18r_0\varepsilon^5)}{r_0(\varepsilon+1)^2(3r_0+3r_0\varepsilon-4\xi\chi a)^3(\varepsilon^2+2\varepsilon+\tan^2\alpha+1)^2} \tag{13}$$

$$P = \xi\vec{H}_0^2\chi^2\pi^2a^3\phi\mu_0$$

$$A = (8-20\tan^2\alpha-4\tan^4\alpha)\xi\chi a+(9\tan^2\alpha+9\tan^4\alpha-18)r_0$$

$$B = 27r_0\tan^2\alpha+9r_0\tan^4\alpha-90r_0+32\xi\chi a-40\xi\chi a\tan^2\alpha$$

$$C = 27r_0\tan^2\alpha-180r_0+48\xi\chi a-20\xi\chi a\tan^2\alpha$$

$$D = 9r_0\tan^2\alpha-180r_0+32\xi\chi a$$

To simplify the magneto-induced stress function, the extracted parameters A, B, C, and D are related to tilt angle α that can exhibit strong nonlinear characteristics. The parameter P shows the magnetic properties and size of the particles. The magneto-induced stress function contains high-order exponential terms in order to ensure the accuracy of the model. It is assumed that the higher-order terms above the third orders of the compressive strain can be omitted as infinite terms compared to other terms. The magnetic-induced stress function is expressed as Eqn. (14).

$$\sigma_m = \frac{-0.304P(A+B\varepsilon+C\varepsilon^2+D\varepsilon^3)}{r_0(\varepsilon+1)^2(3r_0+3r_0\varepsilon-4\xi\chi a)^3(\varepsilon^2+2\varepsilon+\tan^2\alpha+1)^2} \tag{14}$$

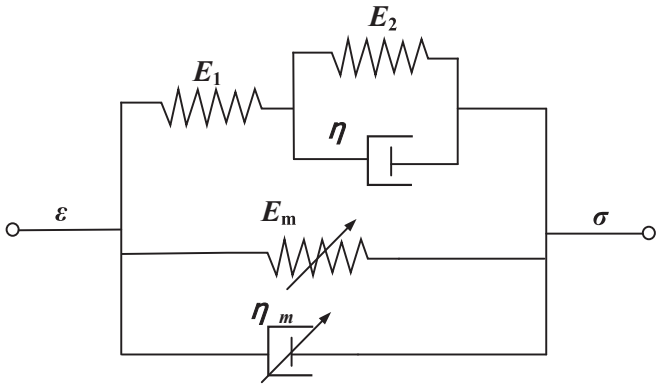

Fig. 4. The modified Kelvin magneto-viscoelasticity model.

The magnetic-induced modulus under compression can be deduced by the second partial derivative of the magnetic energy density function or first partial derivatives of the magneto-induced stress function to the compressive strain, which is shown as Eqn. (15).

$$E_m = \frac{\partial^2 W_m}{\partial\varepsilon^2} = \frac{\partial\sigma_m}{\partial\varepsilon} \tag{15}$$

Thus, the theoretical equation for the compressive magnetic-induced modulus of MREs with tilt angle of magnetic chain is shown as Eqn. (16):

$$\begin{aligned} E_m = {} & \frac{342Pr_0(\varepsilon+1)\left(D\varepsilon^3+C\varepsilon^2+B\varepsilon+A\right)+76P(3r_0+3r_0\varepsilon-4\xi\chi a)\left(D\varepsilon^3+C\varepsilon^2+B\varepsilon+A\right)}{125r_0(\varepsilon+1)^3(3r_0+3r_0\varepsilon-4\xi\chi a)^4\left(\varepsilon^2+2\varepsilon+\tan^2\alpha+1\right)^2} \\ & + \frac{152P(\varepsilon+1)(D\varepsilon^3+C\varepsilon^2+B\varepsilon+A)-38P\left(3D\varepsilon^2+2C\varepsilon+B\right)\left(\varepsilon^2+2\varepsilon+\tan^2\alpha+1\right)}{125r_0(\varepsilon+1)^2(3r_0+3r_0\varepsilon-4\xi\chi a)^3\left(\varepsilon^2+2\varepsilon+\tan^2\alpha+1\right)^3} \end{aligned} \tag{16}$$

The nonlinear mechanical characteristics of the magnetic-induced modulus of the MREs with tilt angle of magnetic chain under compression can be precisely described as Eqn. (16). The magnetic energy of the anisotropic MREs changes significantly under the influence of both the external magnetic field and compressive load. The magneto-mechanical coupling effect of anisotropic MREs cannot be accurately evaluated by the traditional magneto-mechanical model.

The modified Kelvin viscoelasticity model in Fig. 4 is introduced to characterize the dynamic magneto-mechanical properties of the anisotropic MREs under compression mode. The proposed magneto-induced mechanical model of the anisotropic MREs is embedded to obtain the dynamic viscoelastic model. These parameters that are the magneto-induced modulus "E_m" and the dissipation coefficient of magneto-induced "η_m", need to be obtained experimentally for the viscoelastic model shown in Fig. 4. The parameter "η_m", corresponding the dissipation coefficient under a given magnetic field, is obtained by subtracting the area of the hysteresis loop at the magnetic field strength from the area of the hysteresis loop at zero field in compression experiments. The parameter "E_m" presents the difference between the slope of the constitutive-curves under magnetic flux and the slope of the constitutive-curve at zero field, corresponding to compression strain. The E_1, E_2 and η parameters in MREs dynamic viscoelastic model can be identified by using robust fitting method. The magneto-induced modulus E_m in Eqn. (16) is substituted into the Eqn. (A4) in the appendix. η_m obtained in the magneto-mechanical experiments stands the enclosed area of magneto-mechanical hysteresis loop.

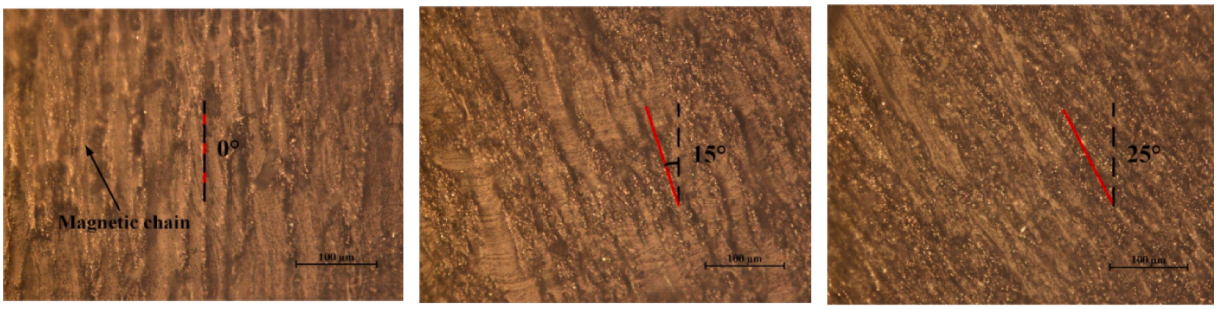

(a) α=0° (b) α=15° (c) α=25°

Fig. 5. The magnetic chain microstructure of anisotropic MREs with tilt angle (φ = 60%).

Table 1
The calculation parameters of theoretical model.

Parameters		Symbols	Reference values
MRE magnetic chain microstructure	The diameter of the particle	$2a$	4–8 μm
	The angle of MRE magnetic chain	α	0-80°
	the reduced spacing of adjacent magnetic dipoles	$r_0/2a$	1.65
Material magnetic properties	Relative permeability of the matrix	μ_l	1
	Vacuum permeability	μ_0	$4\pi \times 10^{-7}$ T•m/A
	Specific magnetization of the CIPs	χ	0.65–3
Carbonyl iron powder mass fraction		φ	60 %, 80%
Compression strain in static mechanics		ε	1%, 5 %

4. Result and discussion

The magneto-induced mechanical model of anisotropic MREs is established based on the magnetic chain microstructure, which provides a theoretical method for characterizing the magneto-induced modulus. The microstructure of magnetic chain was characterized by using the ultra-depth-of-field microscope to obtain the chains morphology of anisotropic MREs with different tilt angles as shown in Fig. 5. Due to the effect of magnetic fields at different angles during the preparation of anisotropic MREs, the magnetic chains are reflected on 0, 15, and 25-degree angles in Fig. 5(a), (b), and (c), which validated reliability of the manufacturing process.

4.1. Theorical analysis of characteristic parameters

The anisotropic MREs with different tilt angles of magnetic chain have special configurations. The microstructural parameters of magnetic chain are subjected to compressive load, which have sensitive changes. The constitutive relation of magneto-induced mechanics presents nonlinear characteristics that mainly reflect on the enhancement effect of magneto-induced modulus. The nonlinear characteristics of magneto-mechanical properties under large compressive deformation cannot be ignored. Thus, the high-order coupling terms of compressive strain, adjacent dipoles spacing and chain tilt angle appear in the theoretical formula (15) of magneto-induced modulus. The analysis results corresponding magneto-induced mechanical model suggest significant effect of anisotropy according to the material parameters of the prepared anisotropic MREs as shown in Table 1. As an example, Fig. 6 shows the influence of the magnetic flux density and the chain tilt angle on the magneto-induced modulus by utilizing the magneto-induced mechanical model of anisotropic MRE.

The comparable trends for the magneto-induced modulus of

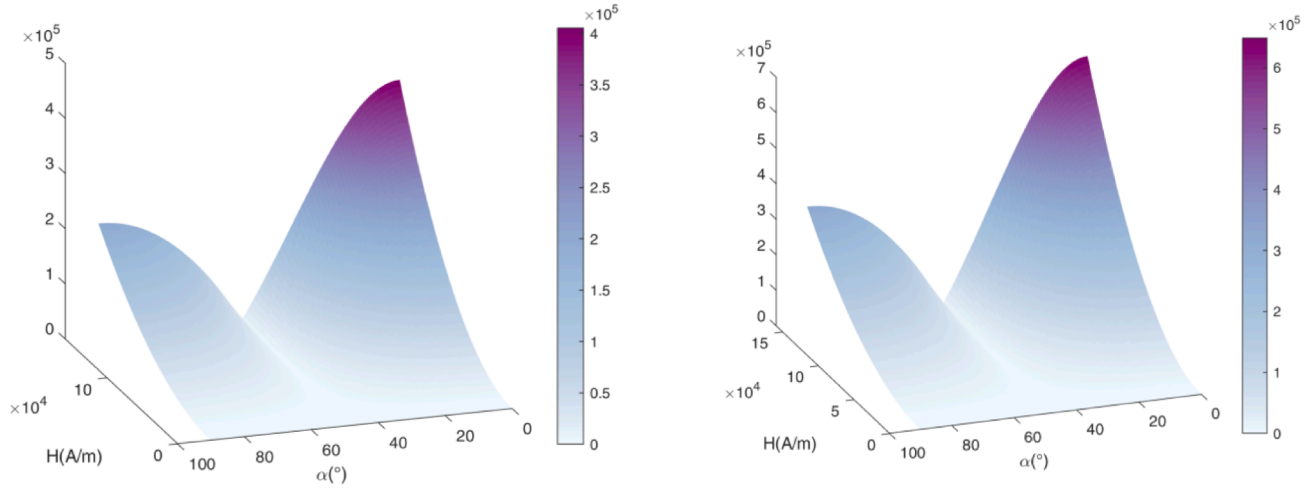

Fig. 6. Influence of tilt angle of magnetic chains on magneto-induced elastic modulus of anisotropic MREs under different compressive strain (a) ε = 1%, φ = 60%; (b) ε = 5%, φ = 60%.

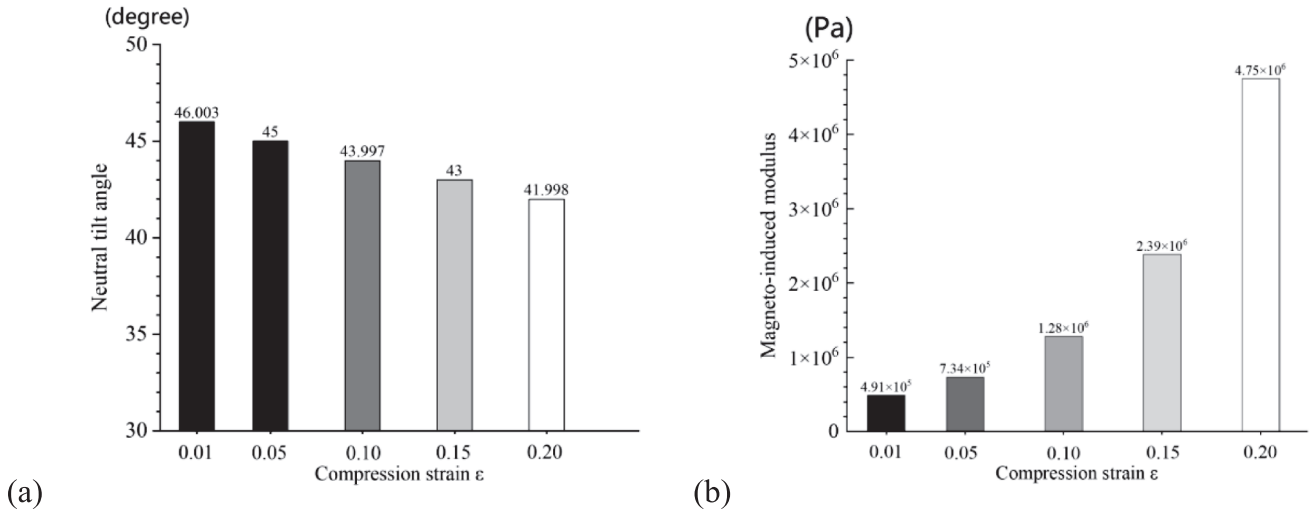

Fig. 7. (a) The neutral tilt angle of magnetic chain; (b) The effect of compressive strain on magneto-induced modulus (B_o = 220mT, φ = 60%).

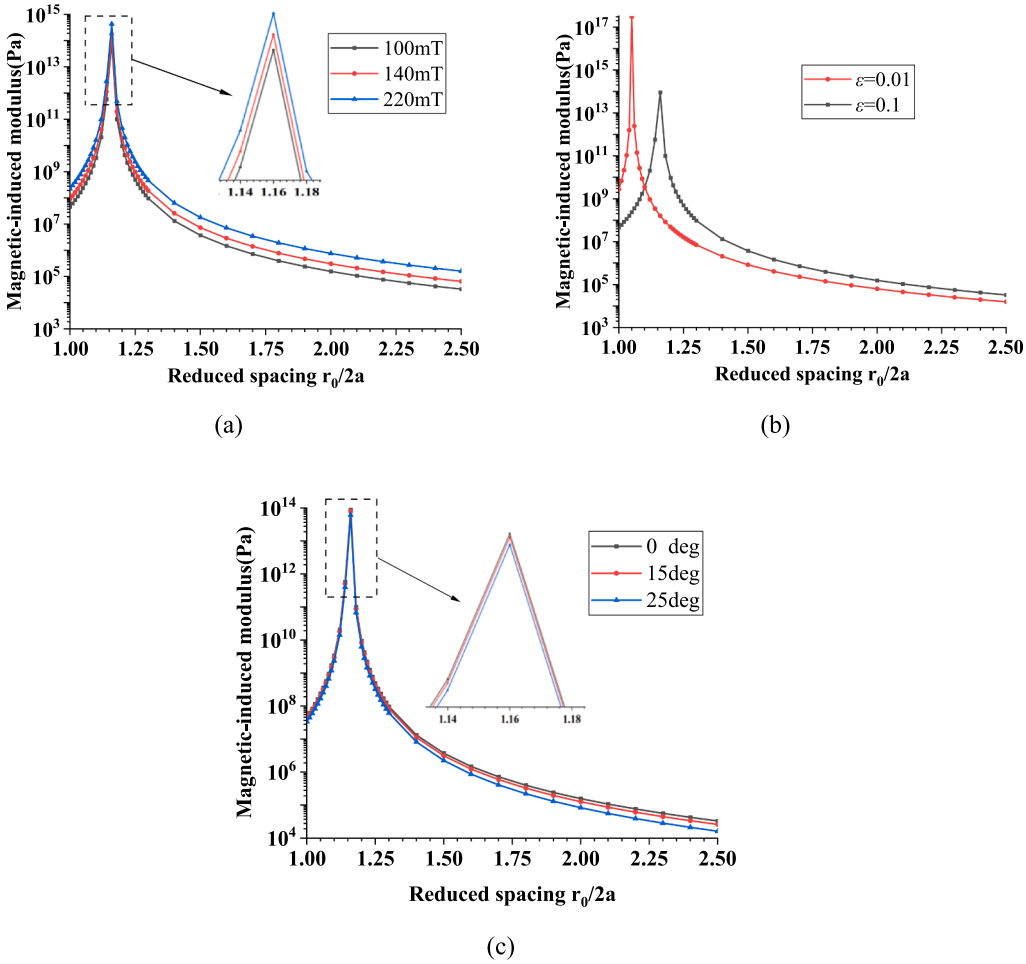

Fig. 8. Effect of the reduced spacing of magnetic dipole on magneto-induced modulus(a) the modulation of magnetic flux density (φ = 55%, ε = 0.1, α = 0°); (b) the modulation of compressive strain (φ = 55%, B_o = 100mT, α = 0°); (c) the modulation of magnetic chain tilt angle (φ = 55%, B_o = 100mT, ε = 0.1).

anisotropic MRE were observed on magnetic flux density and chain tilt angle under different compressive deformation in Fig. 6. The results suggest that magneto-induced modulus of anisotropic MREs is a monotonic change as increasing magnetic flux density in Fig. 7(b). In addition, the magneto-induced modulus firstly decreases and then increases as increasing the tilt angle of magnetic chain. The magneto-mechanical property of anisotropic MRE with tilt angle α, which is neutral angle that is subjected to compression strain, represents the minimum magneto-induced modulus in the entire domain. Theoretically, the maximum value of the chain tilt angle is 90°that the direction of the

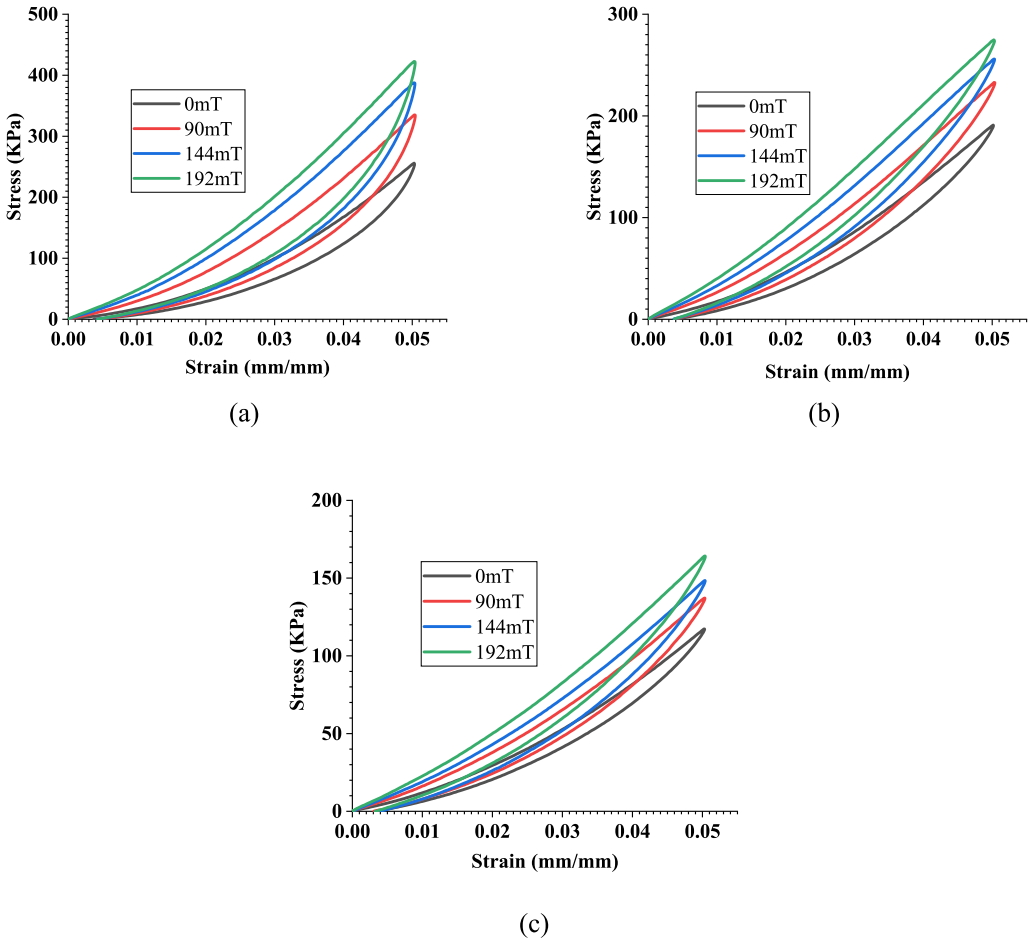

Fig. 9. Effect of magnetic flux density on magneto-mechanical stress–strain curve of anisotropic MREs ($\varphi = 40\%$) with tilt angle of magnetic chain (a) $\alpha = 0°$; (b) $\alpha = 15°$; (c) $\alpha = 25°$.

magnetic chain is perpendicular to the action direction of the magnetic field and compressive load. Fig. 7(a) illustrates smaller neutral tilt angle of anisotropic MREs as increasing the compressive strain.

The dipolar forces between particles in the same chain are decomposed along × axis (F_x) which is the parallel direction of compression surface and z axis (F_z) being the compression and applied field direction. The reason for this phenomenon is that the horizontal component F_x of dipolar forces are balanced each other, thus resulting in a decreasing trend corresponding magneto-induced modulus. The actual tilt angle of magnetic chain becomes larger under compressive deformation by the adjacent magnetic dipoles configuration as shown in Fig. 3. In summary, the nonlinear magneto-induced mechanical characteristics of anisotropic MRE are mainly affected by both the chain microstructure parameters and the compressive strain.

Furthermore, the tendency demonstrates the influence of magnetic flux density, compression strain and chain tilt angle on the relationship between magneto-induced modulus and the reduced spacing. This facilitates the understanding of the mechanism of the magneto-induced mechanics as shown in Fig. 8. When the reduced spacing $r_0/2\mathbf{a} = 1$ indicates the contact arrangement of two adjacent magnetic dipoles in the same magnetic chain. The magneto-induced modulus appears gradually decrease after a sharp increase with the increase of the reduced spacing in Fig. 8(a)(b)(c). The reason for the peaks of these curves is that the interaction of the dipoles arranged on the magnetic chain produces the magnetic dipole moment in the Z-direction. The magnetic energy of the adjacent dipoles is obtained from Eqn. (1), which determines the magneto-induced modulus. The adjacent magnetic dipole spacing $r = r_0(1 + \varepsilon)$ for expression form $1/r^3$ in Eqn. (6), can be processed on both sides to obtain $r/2\mathbf{a} = r0(1 + \varepsilon)/2\mathbf{a}$. So, the magnetic energy of the adjacent dipoles calculated by Eqn. (6) has a maximum value, which is affected by the compression strain. When the compression strain increases, keeping the same $r/2\mathbf{a}$, the corresponding the reduced spacing $r_0/2\mathbf{a}$ increases, as shown by the shift in the curve peak. The results show larger flux density corresponding to a stronger magneto-induced modulus with the increase of the reduced spacing in Fig. 8(a). The compressive strain is applied to constitute the model. The trend of the magneto-induced modulus represents the peak reduction and shifting with increasing the reduced spacing in Fig. 8(b). The magneto-induced modulus gradually stabilizes when the reduced spacing is greater than 1.5. The dipolar interaction has a weaker form at larger the reduced spacing due to magnetic particle with micron-sized volume. As to the value of the magneto-induced modulus at peaks, though theoretically existent, we cannot easily verify its existence, and it is unlikely that the material process can be controlled so precisely. Fig. 8(c) illustrates the effect of magnetic chain tilt angle on the magneto-induced modulus corresponding to the increase of reduced spacing. The magneto-induced modulus slightly decreases in the overall range corresponding to the increase of the tilt angle. The reduced spacing affects the magnetization properties of the magnetic chains in MREs, which in turn leads to influence the magneto-induced mechanical properties of the MREs. The reduced spacing of adjacent dipoles r_0/a is defined to describe the mean gap between adjacent magnetic dipoles in a chain. The reduced spacing is shown in Tab. 1 referring to the preparation process of anisotropic MREs under the magnetic flux density of 1 T.

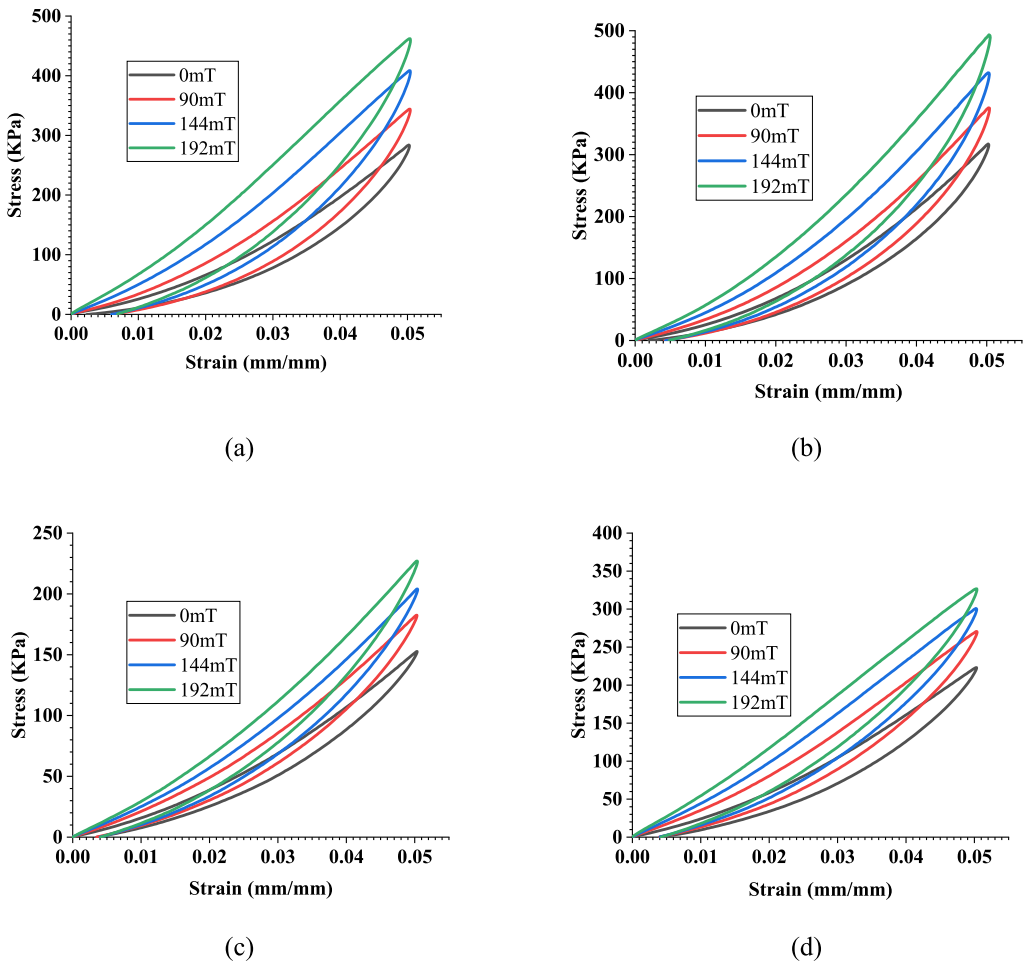

Fig. 10. Effect of magnetic flux density on magneto-mechanical stress–strain curves of anisotropic MREs of different CIPs mass fraction with tilt angles of magnetic chain (a) $\alpha = 15°$, $\varphi = 60\%$; (b) $\alpha = 15°$, $\varphi = 80\%$; (c) $\alpha = 25°$, $\varphi = 60\%$; (d) $\alpha = 25°$, $\varphi = 80\%$.

4.2. Magnetic field effect

The anisotropic MREs with different tilt angles of magnetic chain and mass fractions were tested by using compressive coil of customized design generating perpendicular magnetic fields to obtain hysteresis constitutive curves. Fig. 9 illustrates the effect of magnetic flux density on the compressive hysteresis loops of anisotropic MREs (40% mass fraction) with 0°, 15° and 25° tilt angles at 5% strain. The results are presented for different magnetic flux densities that the influence of tilt angles of magnetic chain on the major axis slope and the enclosed area of hysteresis loops. These suggest magnetic field stiffening of anisotropic MREs, which shows the increase of stress–strain curves slopes for magnetorheological effect.

The slope of the hysteresis curve, presented the elastic modulus of MRE under magnetic field, significantly increase with increasing magnetic flux at same material parameters, including tilt angle and mass fraction. The rate of slope represents the growth rate of the elastic modulus increase, as the compressive strain of MRE under the magnetic flux density increases, which reflects the nonlinear increase in the magneto-elastic stress in Eqn. (13). The magneto-mechanical hysteresis loops are subjected to the tilt angle of magnetic chain in MRE microstructural design. The slope of hysteresis loops decreases more sharply corresponding to increasing the tilt angles of magnetic chain. This is due to dipolar forces (F_z, loading direction) of the CIPs magnetic chain decreasing as the tilt angle of magnetic chain increasing. The sequentially arranged dipoles of magnetic chain of anisotropic MREs increase the attraction in same chain under higher magnetic field intensity. The results show that become greater stiffening under compressive load and

Table 2
Viscoelastic and magneto-induced modulus of anisotropic MREs in experimental results (Pa).

Parameters	Young modulus	Magneto-induced modulus E_m			Loss modulus	Kelvin-Voigt model		
φ / α/ ϕ		90mT	144mT	192mT		E1	E2	η
40%/0°/13.9%	1.03×10^7	1.268×10^6	2.058×10^6	2.348×10^6	2.10×10^6	1.57×10^6	3.18	3.95
40%/15°/13.9%	4.51×10^6	8.334×10^5	1.297×10^6	1.663×10^6	1.47×10^5	1.68×10^6	3.67	4.28
40%/25°/13.9%	4.03×10^6	4.064×10^5	6.32×10^5	9.458×10^5	5.92×10^6	1.76×10^6	3.92	5.16
60%/0°/26.7%	2.64×10^7	1.580×10^6	2.634×10^6	3.333×10^6	4.16×10^6	1.68×10^6	3.78	5.96
60%/15°/26.7%	7.88×10^6	1.218×10^6	2.483×10^6	3.578×10^6	6.94×10^5	1.71×10^6	3.12	6.54
60%/25°/26.7%	7.82×10^6	5.972×10^5	1.028×10^6	1.487×10^6	1.01×10^6	1.95×10^6	2.85	6.78
80%/0°/49.2%	3.63×10^7	2.882×10^6	5.569×10^6	8.073×10^6	6.15×10^6	1.68×10^6	4.25	7.82
80%/15°/49.2%	1.29×10^7	1.453×10^6	2.887×10^6	3.924×10^6	2.61×10^6	1.75×10^6	5.98	8.12
80%/25°/49.2%	9.08×10^6	9.434×10^5	1.554×10^6	2.07×10^6	1.32×10^6	2.16×10^6	6.25	8.89

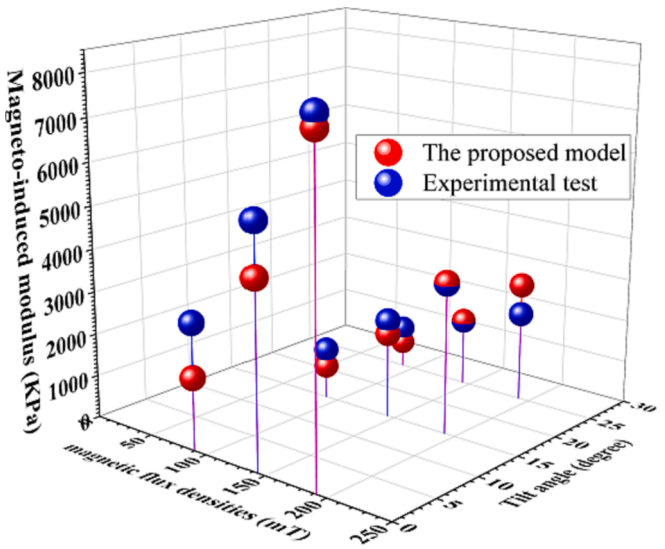

Fig. 11. Comparison between experimental data and model for magneto-induced modulus ($\varphi = 80\%$, $\varepsilon = 5\%$).

the magnetic stress increase sharply.

In addition, this magnetorheological effect is relation with the enclosed area of hysteresis loops, which suggest the influence of the tilt angle of magnetic chain on the energy dissipation under magnetic flux density. Smaller tilt angle of magnetic chain can lead to lower energy dissipation as shown in Fig. 9. Therefore, the design mechanism of magnetic chain is utilized by achieving field-controllable modulation, containing stiffness and damping properties of anisotropic MREs.

The magnetorheological effect is enhanced under increasing the mass fraction of anisotropic MRE without tilt angle, however, decrease with increasing tilt angle of magnetic chain, which propose a magnetorheological controllable mechanism of different directions. The tilt angle of the prepared anisotropic MREs in the study is smaller than the neutral angle, so the experimental results under compression are consistent with the model prediction of the magneto-induced modulus. Furthermore, the increasing of mass fraction of anisotropic MREs is considered for discussing the effect of both chain tilt angle and CIPs mass fraction on the equivalent stiffness and energy dissipation. The regulation of equivalent stiffness is revealed by modifying mass fraction and tilt angle, when compared to the anisotropic MRE, as seen in Fig. 10(a) (c) and (d). The results show the range decrease (from 178 kPa to 74.6 kPa) of magneto-induced stress when the tilt angle of magnetic chain increasing corresponding to 60% CIPs mass fraction. The simultaneously increase of mass fraction and tilt angle balance the decrease of magneto-induced modulus due to increasing tilt angle, corresponding to 102.8 kPa for the MRE of $\alpha = 25^{\circ}$ and $\varphi = 80\%$. A tabular summary (Table 2) of the various experimentally obtained moduli of anisotropic MREs is presented, containing Young modulus, magneto-induced modulus and loss modulus. The loss modulus is determined from dynamic properties of anisotropic MREs in section 4.4. The corresponding viscoelastic model parameters for magnetorheological elastomeric materials with

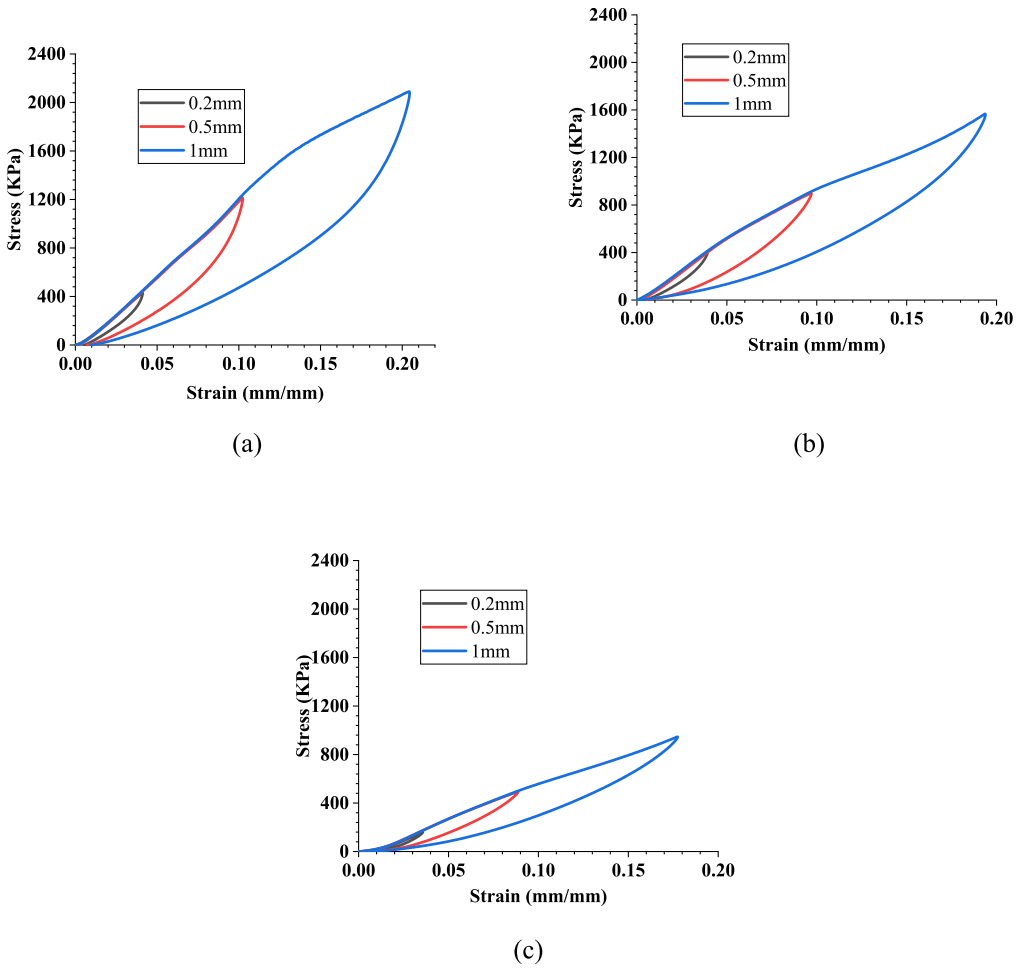

Fig. 12. Schematic of stress–strain hysteresis loops of anisotropic MREs ($\varphi = 60\%$) with tilt angle of magnetic chain for Mullins effects (a) $\alpha = 0^{\circ}$; (b) $\alpha = 15^{\circ}$; (c) $\alpha = 25^{\circ}$.

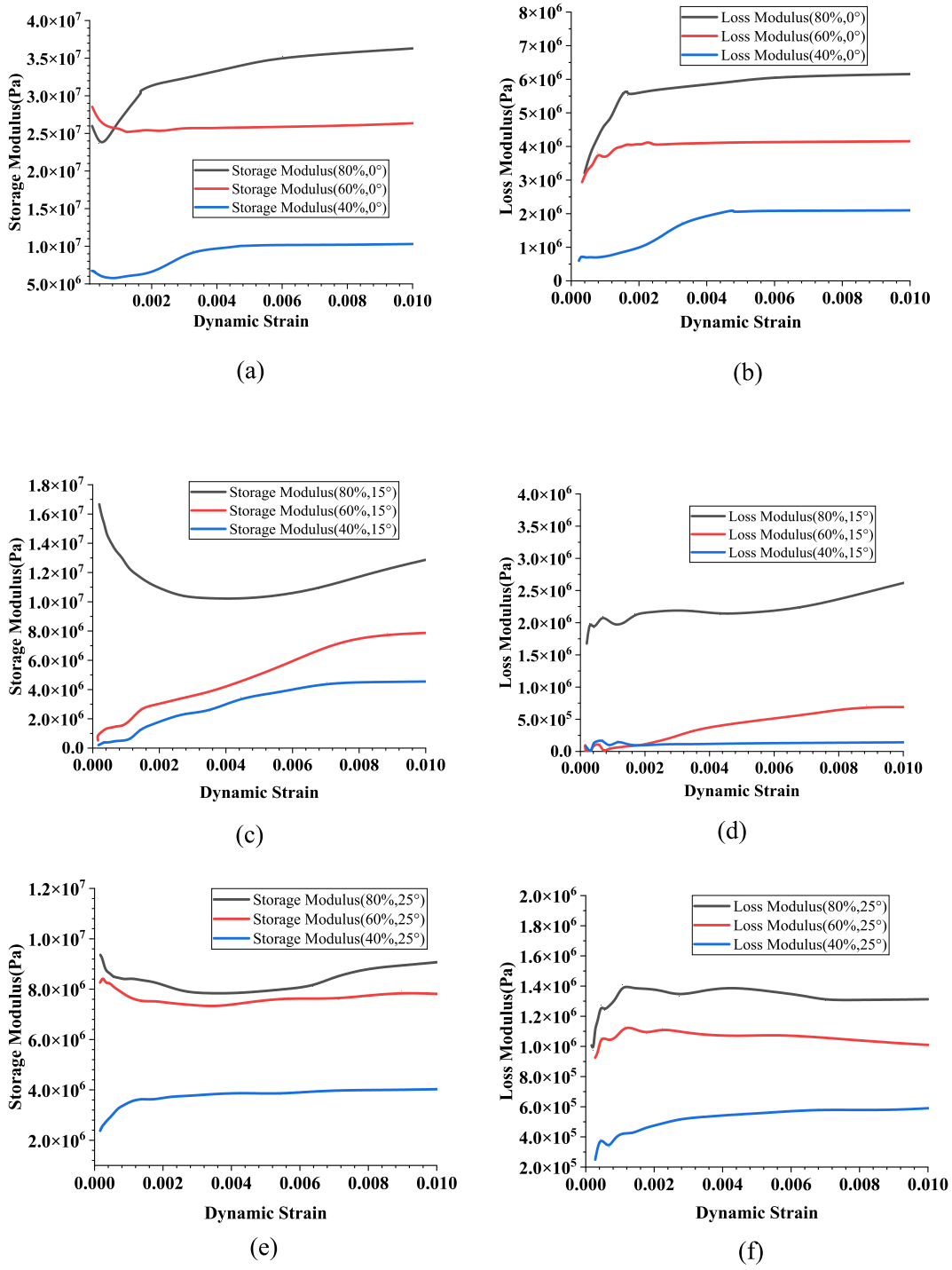

Fig. 13. Dynamic modulus of anisotropic MREs with tilt angle of magnetic chain under different strains amplitude (f = 5 Hz).

different volume fractions and chain tilt angles are also shown in Table 2, containing E1, E2, and η.

In order to evaluate the performance of the proposed model of anisotropic microstructure, the compression modulus obtained from the models are compared with these experimentally measured in Fig. 11. Parameters used in theoretical calculations are listed in Tab. 1. The modeling results showed that the magneto-induced compression modulus of all samples increased with magnetic flux density. The theoretical results and experimental results were fitting well, which consider tilt angle of magnetic chain and CIPs mass fraction. As above mentioned, experimental tests have been performed within the tilt angles of magnetic chain in the range of 40%-80% mass fraction CIPs. The proposed model presents a compression elastic modulus that is independent of excitation frequency. In reference [34], magneto-mechanical elastic modulus of anisotropic MREs under different excitation frequencies are less affected, however, the isotropic MREs are relatively sensitive for strain-rate effect. Therefore, the quasi-static compressive mechanical testing was utilized by using Instron E10K equipment to characterize magneto-induced modulus. The anisotropic MREs with special mechanical properties of magnetic field dependent have consideration of the preparation process to obtain reasonable magnetic dipole spacing.

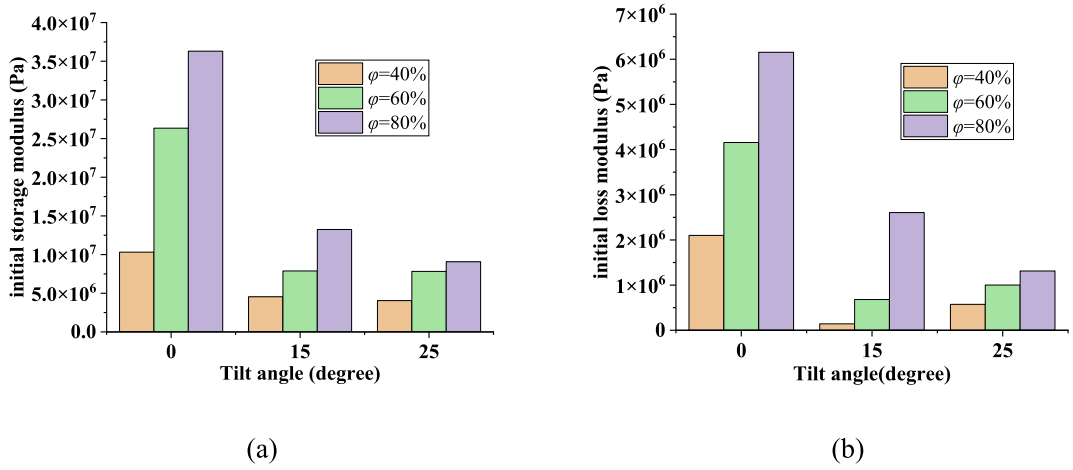

Fig. 14. The dynamic modulus of anisotropic MREs at different tilt angles under zero-field (ε = 1%) (a) Initial storage modulus; (b) Initial loss modulus.

4.3. *Mullins effects*

The hysteresis loops of Mullins effects were investigated for anisotropic MREs with tilt angle of magnetic chain. The strain of the MREs increases with increasing stress along the loading direction as shown in Fig. 12. These curves in Fig. 12 are marked to represent the maximum displacement of the compression experiment, including 0.2, 0.5 and 1 mm. When the stress reaches the peak, the MREs produce softening during unloading, which isn't return along the original path due to the Mullins effect. The different displacement of anisotropic MREs were discussed for the sample of 60% mass fraction CIPs as an example. Similar trend of increasing energy dissipation could be observed when the compression displacement increases in Fig. 12. However, the rate of change of energy dissipation within increasing the tilt angle of magnetic chain, is smaller at larger deformation which means higher rheological effect for smaller tilt angle. The absent magnetic field dependent

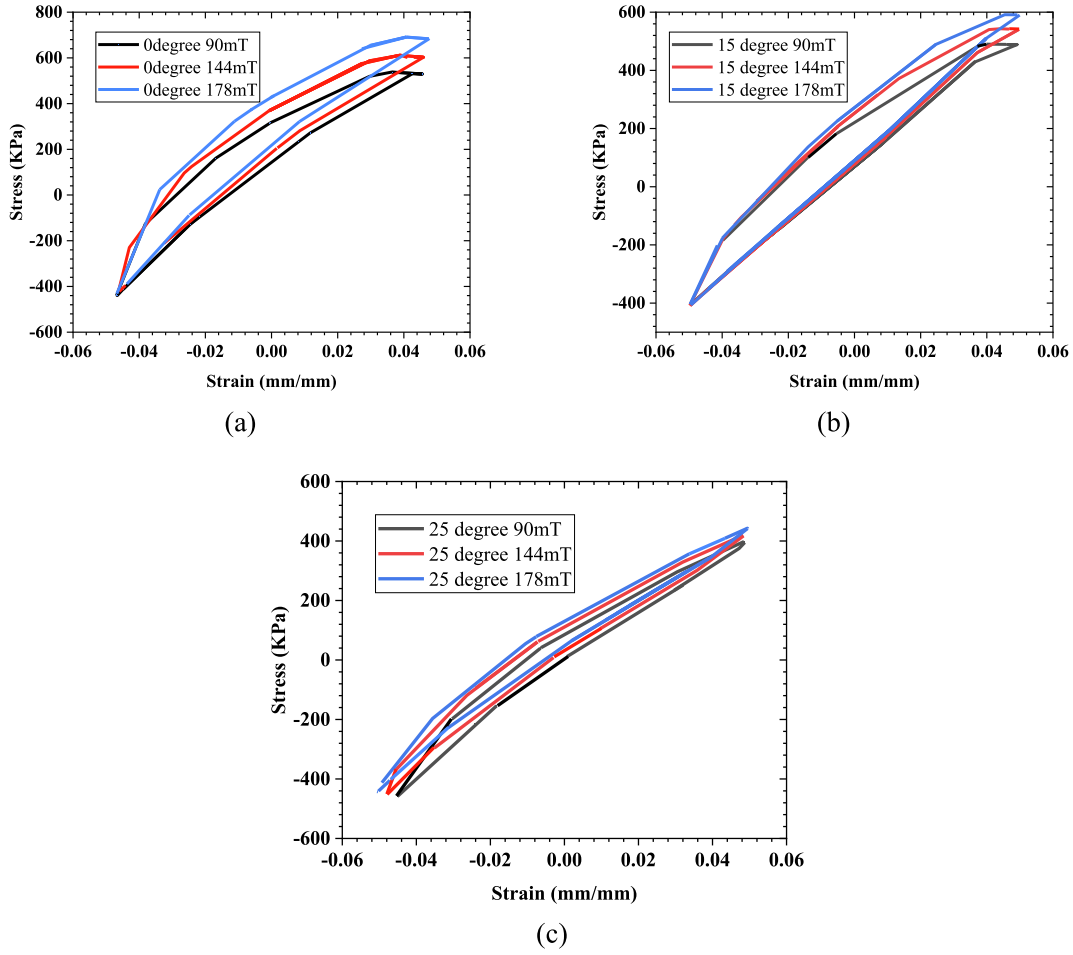

Fig. 15. Dynamic magneto-mechanical hysteresis loop of anisotropic MREs (60%, 10 Hz) under different magnetic flux (a) α = 0° tilt angle; (b) α = 15° tilt angle; (c) α = 25° tilt angle.

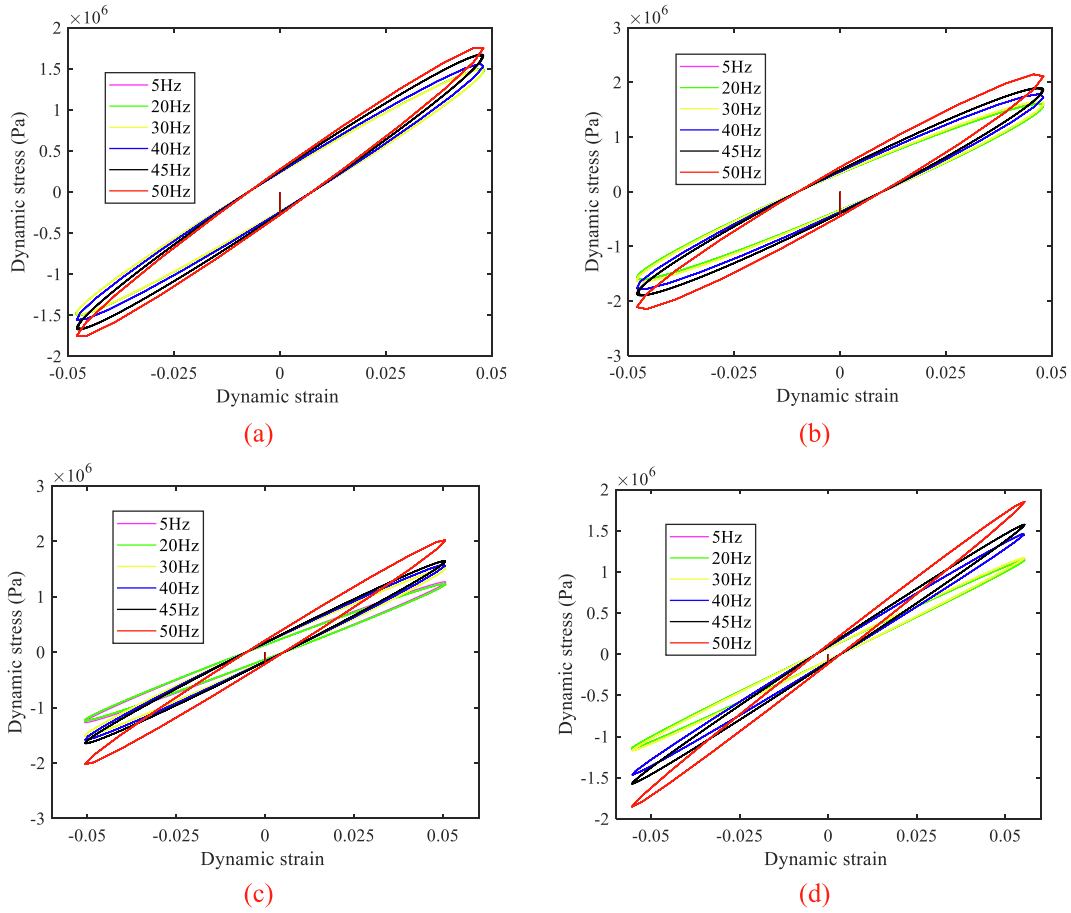

Fig. 16. Dynamic magneto-mechanical hysteresis loop under different frequencies (φ = 60%) (a) α = 0°, B = 90mT; (b) α = 0°, B = 178mT; (c) α = 15°, B = 90mT; (d) α = 25°, B = 90mT.

stiffness and damping properties of anisotropic MREs with the tilt angle, can be used to develop MRE-based smart devices in many engineering applications.

4.4. Dynamic properties of anisotropic MREs

The experiments were designed for characterization of dynamic properties of anisotropic MRE samples with tilt angle in compression mode on basis of standardized methods described in ISO 7743. The complex modulus of anisotropic MREs under compression was tested by using dynamic mechanical analyzer (DMA). The dynamic compressive experiments mainly characterize the complex modulus using 0–1% strain scan as shown in Fig. 13. The results present the effect of the magnetic chain tilt angle, strain amplitude and CIPs mass fraction on the dynamic mechanical properties of anisotropic MREs under compression mode.

The storage modulus at 60% mass fraction has large fluctuations as increasing dynamic strain amplitude, corresponding to the anisotropic MRE of 15-degree tilt angle, observed in Fig. 13(c). Since the strain amplitude is less than 1%, anisotropic MREs has not reached yield deformation. Therefore, the variations in storage modulus are significantly different from the Payne effect [28] produced after yield deformation. The anisotropic MREs of 80% mass fraction with chain tilt angles of 0, 15 and 25°show a dynamic trend for storage modulus that is decreasing and then gradually increasing compared to Fig. 13(a), (c) and (e). The storage modulus of anisotropic MREs with 25-degree tilt angles show the stability region during 0.4–1% strain amplitude in Fig. 13(e). There is a negative correlation for the enhancement of magneto-rheological effect, corresponding to anisotropic MREs with larger tilt angle, by increasing the mass fraction of magnetic particles, as an example in Fig. 13(e) and (f). The trend of loss modulus of anisotropic MREs at different chain tilt angles is presented for gradually increasing over the ranges of 0 ~ 0.3% strain amplitude in Fig. 13(b), (d) and (f). The increases of chain tilt angle of anisotropic MREs presented smaller loss modulus. The tilt angle of magnetic chains in anisotropic MREs is a significant parameter for the microstructure design.

The dynamic modulus at 1% dynamic strain amplitude was extracted for the parameter analysis in the compressive mode as shown in Fig. 14. The storage modulus gradually decreases with the increase of the chain tilt angle, which gradually weakens the contribution of the mass fraction of magnetic particles to the storage modulus. The loss modulus decreases rapidly and then increases slightly at anisotropic MRE of 40% and 60% mass fractions corresponding to the increase of chain tilt angle. In summary, the loss modulus of anisotropic MRE decreases gradually with increasing tilt angles. The loss modulus of anisotropic MRE with 15 and 25°is much lower compared to the MRE with 0-degree magnetic chain in Fig. 14(b).

Fig. 15 demonstrates the effect of magnetic flux density on the stress–strain response of anisotropic MREs with different tilt angles of magnetic chain, corresponding to 5% strain amplitude and frequency 10 Hz. The results show that the slope and the enclosed area of the hysteresis loops as increasing in magnetic flux density, however, the tilt angle of anisotropic MREs increase leading to the slope and the enclosed area decreasing. These suggest magnetic field stiffening and tilt angle softening of the MREs similar to the results of quasi static testing.

The effect of excitation frequency on the dynamic mechanical properties of anisotropic MREs with tilt angles of magnetic chain was investigated. The results, presented in Fig. 16 for $f = 5 \sim 50$ Hz and $\varepsilon =$

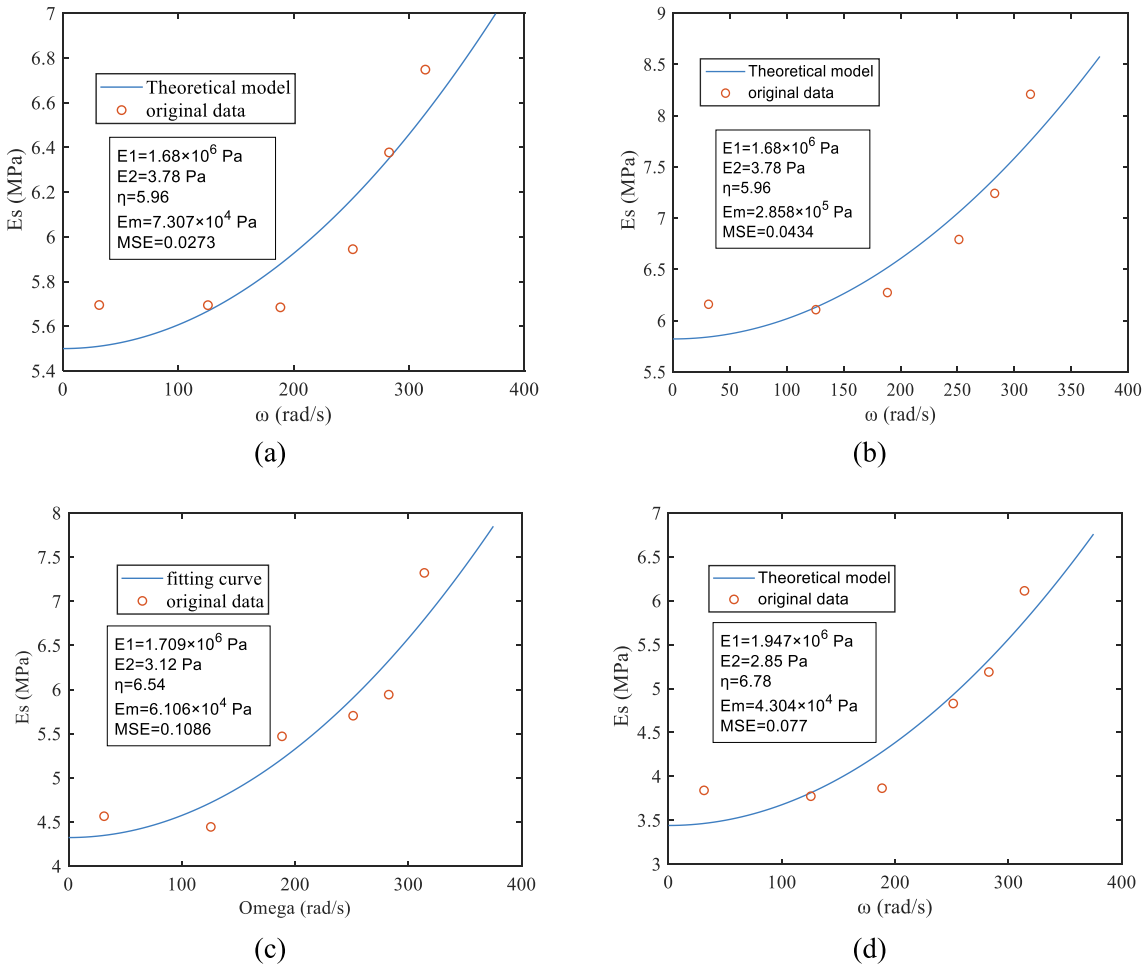

Fig. 17. Dynamic magneto-mechanical storage modulus of anisotropic MRE (60% mass fraction) under different frequencies (a) α = 0°, B = 90mT; (b) α = 0°, B = 178mT; (c) α = 15°, B = 90mT; (d) α = 25°, B = 90mT.

5%, show that the slope of hysteresis loop of those MREs with tilt angle slightly decreases and then significantly increases as rising excitation frequency. As an example, Fig. 16(a) and (b) compare the magneto-mechanical property of the anisotropic MRE with 0-degree magnetic chain under different excitation frequencies, ranging from 5 to 50 Hz. The results, corresponding to magnetic flux densities of B = 90 mT and B = 178 mT, demonstrate increase in the slope of hysteresis loop with higher frequency, which explains a strain-rate stiffening effect [34].

The dependency frequency of the slope of hysteresis loop or equivalent stiffness is relatively large in the case of the anisotropic MREs with larger tilt angle, as shown in Fig. 16(c) and (d). Thus, the excitations frequency at higher level leaded a sensitive effect for the anisotropic MREs with greater tilt angle. In addition, greater tilt angle, however, decreases the energy dissipation by the MRE with 15-degree compared to the MRE with 25-degree. This is consistent with the performance of quasi-static test results.

The dynamic storage modulus Es of anisotropic MREs subjected to magnetic flux and frequency (strain-rate), is evaluated for using the proposed model in the compression mode. The testing data were employed to determine Es using the general method for compression mode of polymers, depicted in ISO 4664–1. The storage modulus is affected by the peaks of dynamic stress and strain. The ratio is the slope of hysteresis loop. Fig. 17(a) and (b) demonstrate variations in the storage modulus of the anisotropic MREs with 0-degree tilt angle under different excitation frequencies and flux densities, respectively. The results show that magnetic flux increasing enhance the stiffening effect for only frequency contribution. Moreover, the trend of storage modulus of anisotropic MREs illustrates nonlinearity in those fitting curves as the angular frequency gradually increasing. Owing to considerable tilt angle of magnetic chain in anisotropic MREs, the results, presented in Fig. 17 (c) and (d) for α = 15° and α = 25° and B = 90 mT, suggest that the effect of frequency or strain-rate on storage modulus under magnetic flux has more significant performance on rheological effect.

The double square formula as weight function for robust fitting method was used to verify the improved Kevin viscoelasticity model, incorporated the proposed magneto-induced model. The results show the high accuracy of nonlinear fitting in all conditions, the mean square error (MSE) presented for the maximum 0.108 and the minimum 0.027. These results also confirm that the proposed magneto-induced mechanical model is suitable for dynamic mechanical model. Kelvin-Voigt viscoelastic model belongs to the category of phenomenological model, arising from experimental results. The viscoelastic parameters are expressed as the elastic spring part and viscous damping part of the macroscopic material in the combined form. The units of E1 and E2 are Pascal. This is different from the bulk phase based mechanical modeling of elastic composites.

5. Conclusions

In this study, the magneto-mechanical properties of anisotropic MREs with different tilt angles of magnetic chain under quasi-static and dynamic compression deformation were experimentally investigated. Experimental characterization in compression mode was carried out by using the customized coil with compressive head. The results illustrated

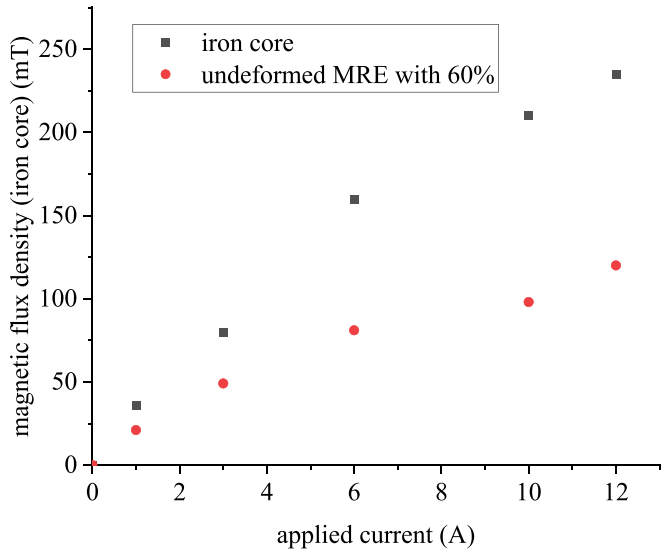

Fig. A1. Correlation of magnetic flux and applied current for surface of iron core and MRE (φ = 60%).

that larger the tilt angle of magnetic chain lead to the smaller magneto-induced modulus under compression mode. Theoretical model was performed based on microscale modeling approach considering the tilt angle of magnetic chain and compressive strain. The proposed model, incorporating modified magnetic dipole theoretical model, was used to validate the experimental results. The neutral tilt angle of magnetic chain in anisotropic MRE present the minimum of magneto-induced modulus over the range. Those anisotropic MREs under magnetic field, were discussed for the influence of the tilt angle, dipoles reduced spacing and compression strain on magneto-induced modulus. The compression deformation is beneficial for the enhancement of the magneto-induced modulus of the MREs.

Furthermore, the experimental investigation has been conducted for the effects of those parameters on dynamic mechanical properties. This mechanism of microstructure design facilitates the regulation of the magnetorheological effect, which present stiffness and damping decreasing. The results show a significant effect on the zero-field modulus of anisotropic MREs, presented for dynamic strain scanning, that decreases sharply as the increase of tilt angle of magnetic chain. The influence of frequency or strain-rate on the dynamic magneto-mechanical property of anisotropic MREs under compression mode was analyzed for different tilt angles of magnetic chain. The improved Kelvin viscoelastic model in Appendix, incorporating the proposed model, was employed as describing dynamic magneto-mechanical property of the anisotropic MREs. The experimental results were well fitting in the improved Kelvin model, which show that the mean square error (MSE) is between 0.0273 and 0.1086. Thus, the proposed magneto-induced mechanical model of anisotropic MRE has potential applications for mechanical metamaterials, adaptive vibration absorbers, soft body robotics, and prosthetic devices etc.

CRediT authorship contribution statement

Leizhi Wang: Conceptualization, Methodology, Writing – original draft. **Zhaobo Chen:** Supervision, Writing – review & editing. **Like Jiang:** Investigation, Visualization. **Li Cheng:** Supervision, Writing – review & editing.

Declaration of Competing Interest

The authors declare the following financial interests/personal relationships which may be considered as potential competing interests: 'Zhaobo CHEN, Leizhi WANG reports was provided by Harbin Institute of Technology. Leizhi WANG reports financial support was provided by The Hong Kong Polytechnic University.'

Data availability

No data was used for the research described in the article.

Acknowledgements

Financial support from the National Key R&D Program of China (2019YFE0116200) and Central Research Grant (CRG) of Hong Kong PolyU, and the supervision and revision support from Prof. Li Cheng and Prof. Zhaobo Chen are gratefully acknowledged.

Appendix

In Eqn. (A1), E1 and E2 present elastic parameters in the modified Kelvin magneto-viscoelasticity model; η is the inherent viscoelastic coefficient and η_m is magneto-induced viscoelastic coefficient corresponding to the damping loss. σ_{ve} and ε_{ve} represent the dynamic stress and dynamic strain in the viscoelastic model, respectively. ψ is a phase difference between strain wave and stress wave in Eqn. (A2). ω is angular frequencies in following equations.

$$(E_1+E_2)\sigma_{ve}+\eta\dot{\sigma}_{ve}=(E_1E_2+E_1E_m+E_2E_m)\varepsilon_{ve}+(E_1\eta+E_m\eta+E_1\eta_m+E_2\eta_m)\dot{\varepsilon}_{ve}+\eta\eta_m\ddot{\varepsilon}_{ve} \tag{A1}$$

$$\varepsilon_{ve}(t)=\varepsilon_0e^{i\omega t}=\varepsilon_0(\cos(\omega t)+i\sin(\omega t)) \qquad \sigma_{ve}(t)=\sigma_0e^{i(\omega t+\psi)} \tag{A2}$$

Submitting the alternating strain and stress of dynamic response Eqn. (A2) into viscoelastic constitution differential Eqn. (A1), can obtain stress–strain dynamic response function Eqn. (A3).

$$\sigma_{ve}(t)=\frac{Q^*(i\omega)}{P^*(i\omega)}\varepsilon_0e^{i\omega t}=(E_S(\omega)+iE_L(\omega))\varepsilon_0e^{i\omega t} \tag{A3}$$

E_S and E_L represent the dynamic compression storage modulus and loss modulus, respectively, so the compressive complex modulus is Eqn. (A4).

$$E^*(i\omega)=\frac{E_1E_2+E_1E_m+E_2E_m-\eta\eta_m\omega^2+i(E_1\eta+E_m\eta+E_1\eta_m+E_2\eta_m)\omega}{E_1+E_2+i\eta\omega} \tag{A4}$$

The expressions for the compressive storage modulus and loss modulus are as follows.

$$E_S(\omega)=\frac{(E_1+E_2)(E_1E_2+E_1E_m+E_2E_m)+(E_1+E_m)\eta^2\omega^2}{(E_1+E_2)^2+\eta^2\omega^2} \tag{A5}$$

$$E_L = \frac{\eta^2\eta_m\omega^3 + (E_1+E_2)^2\eta_m\omega^2}{(E_1+E_2)^2 + \eta^2\omega^2} \tag{A6}$$

The loss tangent can present as Eqn. (A7).

$$\tan\delta = \frac{\eta^2\eta_m\omega^3 + E_1^2\eta\omega + (E_1+E_2)^2\eta_m\omega}{(E_1+E_2)(E_1E_2 + E_1E_m + E_2E_m) + (E_1+E_m)\eta^2\omega^2} \tag{A7}$$

In this study, a simple verification of magnetic induction in the selected magnetic field range is shown in Fig. A1, which indicates that the magnetic field does not reach magnetic saturation at about 250 mT. Thus, these provide proof on the validity of the linear magnetic field assumption.

References

[1] S. Sun, H. Deng, J. Yang, W. Li, H. Du, G. Alici, M. Nakano, An adaptive tuned vibration absorber based on multilayered MR elastomers, Smart Mater. Struct. 24 (4) (2015).
[2] Q. Yang, Y. Yang, Q. Wang, L. Peng, Study on the fluctuating wind responses of constructing bridge towers with magnetorheological elastomer variable stiffness tuned mass damper, J. Intell. Mater. Syst. Struct. 33 (2) (2021) 290–308.
[3] G. Liao, X. Gong, S. Xuan, Phase based stiffness tuning algorithm for a magnetorheological elastomer dynamic vibration absorber, Smart Mater. Struct. 23 (1) (2014).
[4] C. Liu, R. Sedaghati, P. Shang, A novel semi-active switching control scheme for magnetorheological elastomer-based vibration isolator under dynamic input saturation, Smart Mater. Struct. 30 (9) (2021).
[5] T. Hu, S. Xuan, L. Ding, X. Gong, Stretchable and magneto-sensitive strain sensor based on silver nanowire-polyurethane sponge enhanced magnetorheological elastomer, Mater. Des. 156 (2018) 528–537.
[6] T. Hu, S. Xuan, L. Ding, X. Gong, Liquid metal circuit based magnetoresistive strain sensor with discriminating magnetic and mechanical sensitivity, Sens. Actuators B 314 (2020).
[7] Y.J. Park, S.B. Choi, A new tactile transfer cell using magnetorheological materials for robot-assisted minimally invasive surgery, Sensors (Basel) 21 (9) (2021).
[8] D.S. Choi, T.H. Kim, S.H. Lee, C. Pang, J.W. Bae, S.Y. Kim, Beyond human hand: shape-adaptive and reversible magnetorheological elastomer-based robot gripper skin, ACS Appl. Mater. Interfaces 12 (39) (2020) 44147–44155.
[9] P. Zhang, M. Kamezaki, Z. He, H. Sakamoto, S. Sugano, EPM–MRE: electropermanent magnet-magnetorheological elastomer for soft actuation system and its application to robotic grasping, IEEE Rob. Autom. Lett. 6 (4) (2021) 8181–8188.
[10] H.J. Chung, A.M. Parsons, L. Zheng, Magnetically controlled soft robotics utilizing elastomers and gels in actuation: a review, Adv. Intelligent Syst. 3 (3) (2020).
[11] S. Liu, S. Wang, S. Xuan, S. Zhang, X. Fan, H. Jiang, P. Song, X. Gong, Highly flexible multilayered e-skins for thermal-magnetic-mechanical triple sensors and intelligent grippers, ACS Appl. Mater. Interfaces 12 (13) (2020) 15675–15685.
[12] Q. Shu, T. Hu, Z. Xu, J. Zhang, X. Fan, X. Gong, S. Xuan, Non-tensile piezoresistive sensor based on coaxial fiber with magnetoactive shell and conductive flax core, Compos. A Appl. Sci. Manuf. 149 (2021).
[13] I. Bica, E.M. Anitas, M. Bunoiu, B. Vatzulik, I. Juganaru, Hybrid magnetorheological elastomer: influence of magnetic field and compression pressure on its electrical conductivity, J. Ind. Eng. Chem. 20 (6) (2014) 3994–3999.
[14] A.K. Bastola, M. Hossain, A review on magneto-mechanical characterizations of magnetorheological elastomers, Compos. B Eng. 200 (2020).
[15] Ubaidillah, J. Sutrisno, A. Purwanto, S.A. Mazlan, Recent progress on magnetorheological solids: materials, fabrication, testing, and applications, Adv. Eng. Mater. 17 (5) (2015) 563–597.
[16] M.R. Jolly, J.D. Carlson, B.C. Muñoz, T.A. Bullions, The magnetoviscoelastic response of elastomer composites consisting of ferrous particles embedded in a polymer matrix, J. Intell. Mater. Syst. Struct. 7 (6) (1996) 613–622.
[17] M.R. Jolly, J.D. Carlson, B.C. Muñoz, A model of the behaviour of magnetorheological materials, Smart Mater. Struct. 5 (5) (1996) 607–614.
[18] Y. Shen, M.F. Golnaraghi, G.R. Heppler, Experimental research and modeling of magnetorheological elastomers, J. Intell. Mater. Syst. Struct. 15 (1) (2016) 27–35.
[19] Y. Han, W. Hong, L.E. Faidley, Field-stiffening effect of magneto-rheological elastomers, Int. J. Solids Struct. 50 (14–15) (2013) 2281–2288.
[20] S. Rudykh, K. Bertoldi, Stability of anisotropic magnetorheological elastomers in finite deformations: a micromechanical approach, J. Mech. Phys. Solids 61 (4) (2013) 949–967.
[21] X. Zhang, W. Li, X.L. Gong, An effective permeability model to predict field-dependent modulus of magnetorheological elastomers, Commun. Nonlinear Sci. Numer. Simul. 13 (9) (2008) 1910–1916.
[22] J. Feng, S. Xuan, T. Liu, L. Ge, L. Yan, H. Zhou, X. Gong, The prestress-dependent mechanical response of magnetorheological elastomers, Smart Mater. Struct. 24 (8) (2015).
[23] D. Ivaneyko, V. Toshchevikov, D. Borin, M. Saphiannikova, G. Heinrich, Mechanical properties of magneto-sensitive elastomers in a homogeneous magnetic field: theory and experiment, Macromol. Symp. 338 (1) (2014) 96–107.
[24] P. Ponte Castañeda, E. Galipeau, Homogenization-based constitutive models for magnetorheological elastomers at finite strain, J. Mech. Phys. Solids 59 (2) (2011) 194–215.
[25] L. Chen, X.L. Gong, W.H. Li, Microstructures and viscoelastic properties of anisotropic magnetorheological elastomers, Smart Mater. Struct. 16 (6) (2007) 2645–2650.
[26] Z. Varga, G. Filipcsei, M. Zrínyi, Magnetic field sensitive functional elastomers with tuneable elastic modulus, Polymer 47 (1) (2006) 227–233.
[27] F. Gordaninejad, X. Wang, P. Mysore, Behavior of thick magnetorheological elastomers, J. Intell. Mater. Syst. Struct. 23 (9) (2012) 1033–1039.
[28] H. Vatandoost, S. Rakheja, R. Sedaghati, Effects of iron particles' volume fraction on compression mode properties of magnetorheological elastomers, J. Magn. Magn. Mater. 522 (2021).
[29] H. Vatandoost, M. Hemmatian, R. Sedaghati, S. Rakheja, Dynamic characterization of isotropic and anisotropic magnetorheological elastomers in the oscillatory squeeze mode superimposed on large static pre-strain, Compos. B Eng. 182 (2020).
[30] S.W. Chen, R. Li, Z. Zhang, X.J. Wang, Micromechanical analysis on tensile modulus of structured magneto-rheological elastomer, Smart Mater. Struct. 25 (3) (2016).
[31] X. Gong, Y. Wang, T. Hu, S. Xuan, Mechanical property and conductivity of a flax fibre weave strengthened magnetorheological elastomer, Smart Mater. Struct. 26 (7) (2017).
[32] G. Schubert, P. Harrison, Large-strain behaviour of Magneto-Rheological Elastomers tested under uniaxial compression and tension, and pure shear deformations, Polym. Test. 42 (2015) 122–134.
[33] I. Agirre-Olabide, M.J. Elejabarrieta, A new magneto-dynamic compression technique for magnetorheological elastomers at high frequencies, Polym. Test. 66 (2018) 114–121.
[34] A.K. Bastola, V.T. Hoang, L. Li, A novel hybrid magnetorheological elastomer developed by 3D printing, Mater. Des. 114 (2017) 391–397.
[35] A.K. Bastola, M. Paudel, L. Li, Development of hybrid magnetorheological elastomers by 3D printing, Polymer 149 (2018) 213–228.
[36] A.K. Bastola, M. Paudel, L. Li, Dot-patterned hybrid magnetorheological elastomer developed by 3D printing, J. Magn. Magn. Mater. 494 (2020).
[37] E. Yarali, et al., Magneto-/electro-responsive polymers toward manufacturing, characterization, and biomedical/soft robotic applications, Appl. Mater. Today 26 (2022), 101306.
[38] H. Vatandoost, M. Hemmatian, R. Sedaghati, S. Rakheja, Effect of shape factor on compression mode dynamic properties of magnetorheological elastomers, J. Intell. Mater. Syst. Struct. 32 (15) (2021) 1678–1699.
[39] H. Vatandoost, S. Rakheja, R. Sedaghati, M. Hemmatian, Compensation of magnetic force of an electromagnet for compression mode characterization of magnetorheological elastomers, IEEE Trans. Magn. 57 (1) (2021) 1–14.
[40] A. Boczkowska, S.F. Awietjan, R. Wroblewski, Microstructure–property relationships of urethane magnetorheological elastomers, Smart Mater. Struct. 16 (5) (2007) 1924–1930.
[41] J. Zhang, H. Pang, Y. Wang, X. Gong, The magneto-mechanical properties of off-axis anisotropic magnetorheological elastomers, Compos. Sci. Technol. 191 (2020).
[42] T. Tian, M. Nakano, Fabrication and characterisation of anisotropic magnetorheological elastomer with 45° iron particle alignment at various silicone oil concentrations, J. Intell. Mater. Syst. Struct. 29 (2) (2017) 151–159.
[43] A. Boczkowska, S.F. Awietjan, S. Pietrzko, K.J. Kurzydłowski, Mechanical properties of magnetorheological elastomers under shear deformation, Compos. B Eng. 43 (2) (2012) 636–640.
[44] S.S. Sun, Y. Chen, J. Yang, T.F. Tian, H.X. Deng, W.H. Li, H. Du, G. Alici, The development of an adaptive tuned magnetorheological elastomer absorber working in squeeze mode, Smart Mater. Struct. 23 (7) (2014).